JOURNAL OF SPACECRAFT AND ROCKETS
Vol. 33, No. 3, May–June 1996

Engineering Notes

ENGINEERING NOTES are short manuscripts describing new developments or important results of a preliminary nature. These Notes cannot exceed 6 manuscript pages and 3 figures; a page of text may be substituted for a figure and vice versa. After informal review by the editors, they may be published within a few months of the date of receipt. Style requirements are the same as for regular contributions (see inside back cover).

Compressibility and Pressure-Gradient Correction Assessment for Turbulent Hypersonic Flows

Jiasen Hu* and Arthur Rizzi†
Royal Institute of Technology, S-100 44 Stockholm, Sweden

Introduction

KNOWLEDGE of the flow development in hypersonic wind-tunnel nozzles is of primary importance to the design of such nozzles as well as to the characterization of the flowfield in the test section. In the perfect-gas regime, reliable numerical methods have been developed for both of the design work and the flow analysis, but there still exist some deficiencies in predicting the turbulent hypersonic nozzle wall boundary layers. This problem is believed to be a consequence of the deficiencies in the compressible eddy-viscosity turbulence models currently adopted in engineering applications. Specifically, to improve the accuracy of such calculations, the importance of compressibility and pressure-gradient effects should be investigated, since the hypersonic wind-tunnel nozzle flow is characterized by the existence of an increasing main flow Mach number and a varying pressure gradient in the streamwise direction.

A numerical study of that nature is presented in this work. Several explicit compressibility and pressure-gradient corrections are introduced to two widely used eddy-viscosity turbulence models for the calculations of hypersonic wind-tunnel nozzle flows. The results are compared with those obtained with the standard models to evaluate the effects of the corrections, and are compared with measurements to verify the accuracy of the calculations and to see the improvements gained.

Numerical Modeling

The study was carried out by solving three-dimensional Reynolds-averaged Navier–Stokes equations. They are the transport equations to describe the conservation of mass, momentum, and energy with the assumption of a perfect gas. When two-equation turbulence models are employed, the system has two more equations for the turbulent kinetic energy k and its dissipation rate ϵ. In the present work the turbulence is closed by four alternative eddy-viscosity models, among which the Baldwin–Lomax algebraic model[1] and the k–ϵ model of Chien[2] are chosen as the baseline models for the purpose of evaluating the compressibility and pressure-gradient corrections. The other two are their modified versions, respectively, with the modifications outlined below.

The modified Baldwin–Lomax model contains two corrections. The first is to modify the closure coefficients c_{cp} and c_{kleb} (Ref. 1) with the values suggested in Ref. 3, i.e., $c_{cp} = 2.0$ and $c_{kleb} = 0.35$, to allow for the increased compressibility in high-speed flows. The second is the use of a modified van Driest's damping factor,[4] $A^+ = 26/(\tau/\tau_w)^{1.7}$, to model the pressure-gradient effects, where τ is the local shear stress and the subscript w means the wall value.

The modifications to the Chien model are concerned with the modeling of the pressure-gradient–velocity term and the mechanism of compressible dissipation. The pressure-gradient–velocity term, representing the effects of a kind of explicit compressibility and the mean-flow pressure gradient, is approximated by the standard gradient transport hypothesis. The compressible dissipation effects are described by the Nichols model.[5] Details of this modified Chien model are given in our original paper.[6]

These four models, i.e., the Baldwin–Lomax model, the Chien k–ϵ model, and their modified versions, will be abbreviated as BL, CH, BL(mod), and CH(mod) hereafter in this Note for convenience.

Computations

The governing equations are solved by a general purpose CFD code called EURANUS.[7] The algorithm is based on a cell-centered finite-volume method. The convective fluxes are computed via the central interpolation with a scalar artificial viscosity. Viscous fluxes and source terms are approximated by a cell-vertex method, and time integration is performed using a four-stage Runge–Kutta scheme.

The nozzle considered is an M7 axisymmetric contoured nozzle installed in a classical low-enthalpy hypersonic wind tunnel at the Aeronautical Research Institute of Sweden. The exit area ratio of the nozzle is 138.9 over a 3.31-m length. Four cases have been calculated, with each of the four turbulence models used, at the stagnation pressure of 1.0×10^7 Pa, stagnation temperature of 580 K, and wall temperature of 353 K. In all of the cases, the turbulent flow starts from the nozzle throat, where the initial boundary-layer profiles are obtained from an upstream laminar solution.

The computational domain is taken as half of the nozzle symmetry plane with a small sector in the spanwise direction. Based on a grid refinement study performed on part of the domain, the final mesh of the whole domain contains $600 \times 116 \times 1$ cells, and the first nodes next to the wall are well located in the viscous sublayer. At the nozzle exit section about 100 cells are inside the experimentally measured boundary layer, and at least 14 cells are in the range of $y^+ \leq 20$ with the first node at $y^+ \approx 0.8$.

Results and Discussion

Presented in Fig. 1 are the boundary-layer profiles obtained at the nozzle exit section where the measurements were taken. For comparison with the experimental data,[8] the radial distance from the wall, denoted by y, is normalized by the local nozzle radius r. The profiles of velocity V, temperature T, and density ρ are normalized by their local centerline values V_c, T_c, and ρ_c, respectively.

As shown in Fig. 1, the two modified models give some substantial changes in the predicted boundary-layer profiles, especially in the Mach-number, temperature, and density distributions. It is clear that the modified models produce fuller Mach-number and velocity profiles in the outer part of the boundary layer, where the resulting temperature decreases and the density increases in comparison with the corresponding baseline solutions. These features are in good agreement with the favorable pressure gradient existing inside the boundary layer, and in accordance with a reduction of the turbulence level observed in the CH(mod) case.[6] Additionally, Fig. 1 shows that the modifications to the BL model have stronger influence

Received June 1, 1995; presented as Paper 95-2313 at the AIAA 26th Fluid Dynamics Conference, San Diego, CA, June 19–22, 1995; revision received Dec. 29, 1995; accepted for publication Jan. 31, 1996.

*Graduate Student, Aeronautical Engineering Division; currently Graduate Student, Division of Heat and Power Technology.

†Professor, Aeronautical Engineering Division. Senior Member AIAA.

Table 1 Errors of computations compared with experiments at nozzle exit

Quantity	Error, %			
	BL	BL(mod)	CH	CH(mod)
δ^*	18.4	1.9	8.0	−0.5
M_c	−2.8	−1.7	−1.9	−1.4

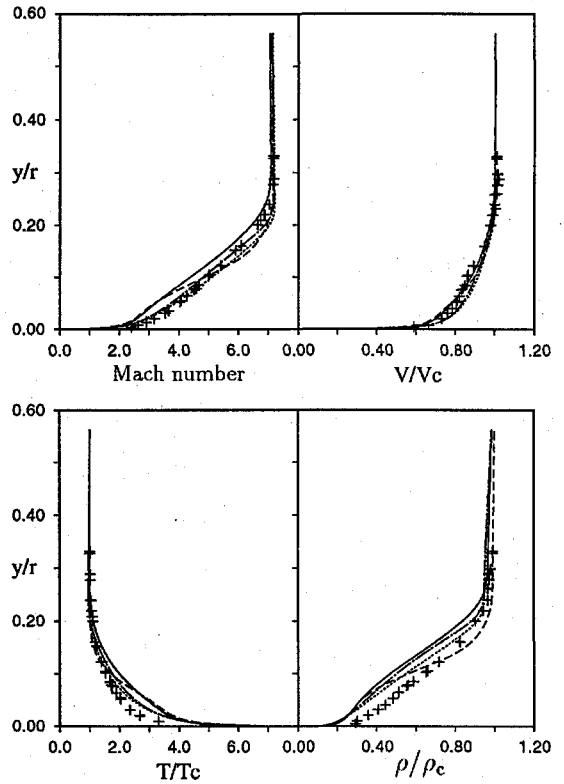

Fig. 1 Boundary-layer profiles at nozzle exit. a) Mach number and velocity and b) temperature and density: ——, BL; – – –, BL(mod); —·—, CH; ····, CH(mod); and +, EXP, Ref. 8.

on the results, except for the velocity profile, than the corrections to the CH model, since more differences have been found between the BL and BL(mod) cases. In the inner region of the boundary layer, however, the modifications to both of the standard models only have quite small effects on the computed results. If compared with the standard models, Fig. 1 shows that both of the modified models can improve the experimental agreement for all the other three profiles to a certain degree, except for the resulting velocity profiles.

Figure 2 displays the axial profiles of boundary-layer displacement thickness δ^*, local skin-friction coefficient c_f, Stanton number St, and centerline Mach number M_c. In the figure each baseline model and its modified version show a similar pattern for each distribution, but the differences in δ^*, c_f, and St are visible. The BL(mod) and CH(mod) can reduce all of these three quantities, but the former makes more changes in the solution. Specifically, the exit δ^*, c_f, and St decrease by 13.9, 29.8, and 30.1%, respectively, on account of the two corrections to the BL model, and by 7.9, 12.2, and 13.6% in the CH(mod) case. For the c_f and St profiles the differences between each standard model and its modified version increase gradually from the nozzle throat, i.e., the transition point, to a certain place in the expansion region, after which the differences remain approximately constant. This phenomenon agrees with the variation of the M_c profiles.

To make the comparison more quantitative, Table 1 gives the relative errors of the calculated δ^* and M_c at the nozzle exit for all the cases. As seen in the table, the improvement due to the corrections in predicting δ^* is notable, and the values of the M_c in the modified cases also have a better experimental agreement than those from the standard cases.

Concluding Remarks

Results of the present work show that including compressibility and pressure-gradient modeling in the type of nozzle simulations investigated can have considerable effects on the computed turbulent boundary layers, and the corrections to the BL model have a stronger influence on the results. Compared with the standard models, both of the modified models can produce improved experimental agreement. But the CH(mod) generally gives a better simulation than the BL(mod). Additionally, the modifications evaluated here are engineering-oriented, are easily implemented, and only slightly

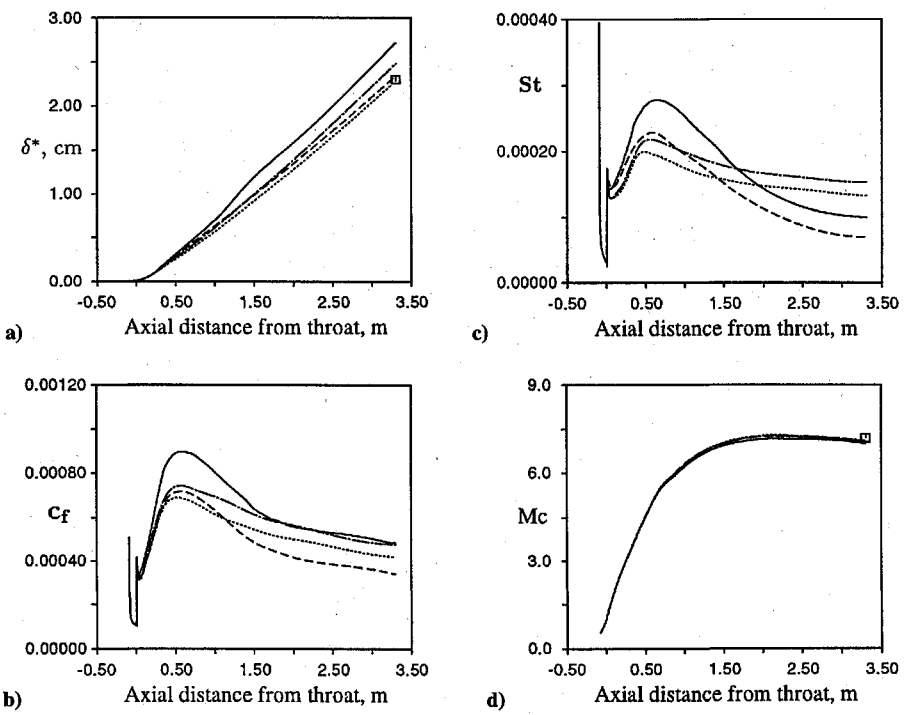

Fig. 2 Axial distributions. a) Boundary-layer displacement thickness, b) local skin-friction coefficient, c) Stanton number, and d) centerline Mach number: ——, BL; – – –, BL (mod); —·—, CH; ····, CH(mod); and □, EXP, Ref. 8.

increase the computational time; therefore, they are applicable for large-scale engineering calculations.

Acknowledgment

This work was partially supported by FFA, the Aeronautical Research Institute of Sweden.

References

[1]Baldwin, B. S., and Lomax, H., "Thin Layer Approximation and Algebraic Model for Separated Turbulent Flow," AIAA Paper 78-257, Jan. 1978.

[2]Chien, K. Y., "Predictions of Channel and Boundary Layer Flows with a Low Reynolds Number Turbulence Model," *AIAA Journal*, Vol. 20, No. 1, 1982, pp. 33–38.

[3]Baysal, O., and Hoffman, W. B., "Simulation of Three-Dimensional Shear Flow Around a Nozzle-Afterbody at High Speeds," *Journal of Fluids Engineering*, Vol. 114, June 1992, pp. 178–185.

[4]Launder, B. E., and Priddin, C. H., "A Comparison of Some Proposals for the Mixing Length Near a Wall," *International Journal of Heat and Mass Transfer*, Vol. 16, No. 3, 1973, pp. 700–702.

[5]Nichols, R. H., "A Two-Equation Model for Compressible Flows," AIAA Paper 90-0494, Jan. 1990.

[6]Hu, J., and Rizzi, A., "Assessment of Compressibility and Pressure-Gradient Corrections for Modeling Turbulent Hypersonic Nozzle Flows," AIAA Paper 95-2313, June 1995.

[7]Rizzi, A., Eliasson, P., Lindblad, I., Hirsch, Ch., Lacor, C., and Haeuser, J., "The Engineering of Multiblock/Multigrid Software for Navier–Stokes Flows on Structured Meshes," *Computers and Fluids*, Vol. 22, No. 2/3, 1993, pp. 341–367.

[8]Hovstadius, G., "Measurement of Boundary Layer Properties in Two Hypersonic Nozzles," Aeronautical Research Inst. of Sweden, FFA Rept. AU-624, Stockholm, Sweden, May 1971.

K. J. Weilmuenster
Associate Editor

Dual-Code Solution Strategy for Hypersonic Flows

William A. Wood* and Richard A. Thompson*
NASA Langley Research Center, Hampton, Virginia 23681-0001
and
Scott Eberhardt†
University of Washington, Seattle, Washington 98195

Nomenclature

C_p	= frozen specific heat at constant pressure, J/kg-K
c	= mass fraction
E_t	= volume-specific total energy, J/m^3
e	= internal energy, (m/s)^2
H	= mixture enthalpy, (m/s)^2
h	= enthalpy, (m/s)^2
h_0	= reference enthalpy at the reference temperature, (m/s)^2
M	= Mach number
$\bar{M}$	= molecular weight, kg/kg-mole
P	= pressure, Pa
q	= heat-transfer rate, W/m^2
R_n	= nose radius, m
$\bar{R}$	= universal gas constant, 8314.3 J/kg-mole-K
T	= temperature, K
u, v, w	= Cartesian velocity components, m/s
X	= axial coordinate, m
α	= angle of attack, deg
ρ	= density, kg/m^3

Subscripts

l	= LAURA
s	= species
u	= UPS
∞	= freestream value

Received June 20, 1995; revision received Nov. 15, 1995; accepted for publication Dec. 11, 1995.

*Aerospace Technologist, Aerothermodynamics Branch, Gas Dynamics Division. Member AIAA.

†Associate Professor, Department of Aeronautics and Astronautics. Member AIAA.

Introduction

INTEREST in reducing the cost of access to space[1] has led to many proposals for advanced launch vehicles that are either fully or partially reusable. Most of these configurations, e.g., the follow-on to Orbital Science's Pegasus[2] and NASA's Single-Stage Vehicle,[1] incorporate slender, blunted configurations. The design process for these vehicles will heavily rely on computational methods to define the aerothermodynamic environment during re-entry.

A popular and proven code developed to solve the re-entry environment is the Navier–Stokes solver Langley Aerothermodynamic Upwind Relaxation Algorithm (LAURA).[3] LAURA is a finite volume, shock-capturing algorithm with second-order spatial accuracy for the steady-state solution of viscous or inviscid hypersonic flows. The scheme employs a point implicit relaxation strategy with upwind-biased flux-difference splitting for perfect gas, equilibrium air, or nonequilibrium air calculations. Although LAURA has successfully computed viscous, reacting flowfields about the Shuttle Orbiter configuration,[4] the time-relaxation approach to solve the thin-layer Navier–Stokes (TLNS) equations can require excessive computational time and memory resources. Several solution strategies have recently been attempted to reduce these computational requirements of a full-vehicle LAURA solution.

Weilmuenster and Gnoffo[5] proposed a multiblock solution procedure, in which the domain is divided into blocks ordered in the streamwise direction. This procedure principally attacks the memory requirements inherent in obtaining a full-body TLNS solution by splitting the domain, but does not decrease the time required to obtain the solution since the TLNS equations remain the governing equations. Greene[6] has extended the LAURA code into a parabolized Navier–Stokes (PNS) version, but this particular formulation, being a TLNS extension, is locally iterative in pseudotime steps, and its performance suffers from arriving as a PNS solver via a TLNS algorithm, rather than being a code that was optimized as a PNS solver from inception. Thus, although this method significantly reduced the memory required to obtain a solution, it was not able to reduce solution time to the level desired.

Upwind parabolized Navier–Stokes Solver (UPS)[7] was identified as a code that, when combined with LAURA, might provide the tremendous reduction in vehicle solution time originally sought with the LAURA–TLNS/LAURA–PNS method. UPS is an upwind, finite volume, state-of-the-art PNS code with perfect gas, equilibrium air, and chemical nonequilibrium capability. It is second-order accurate in the crossflow plane and first-order accurate in the marching direction.

UPS has been used in conjunction with the TLNS code compressible Navier–Stokes solver by Lawrence et al.[8] for perfect gas computations. Nonequilibrium air solutions started from an axisymmetric TLNS code TUFF are presented in Refs. 9–11.

The present study looks to combine two well-established computational codes, LAURA and UPS, for the consistent solution of perfect gas, equilibrium,[12] and chemically reacting hypersonic flowfields. Significantly faster and less costly vehicle aerothermodynamics are sought without compromising the accuracy and sophistication of a full-body LAURA solution. The technique is demonstrated on a blunted, multiconic geometry at angle of attack.

Present Method

The present method seeks to reduce both the computational time and memory associated with obtaining a full-body LAURA solution